Synthesis and Fundamental Studies of Chlorinated Si−Ge Hydride Macromolecules for Strain Engineering and Selective-Area Epitaxial Applications

Jesse B. Tice, Y.-Y. Fang, John Tolle, Andrew Chizmeshya, and J. Kouvetakis*

Department of Chemistry/Biochemistry, Arizona State University, Tempe, Arizona 85287-1604

Received February 12, 2008

We recently demonstrated the low-temperature (400−450 °C) deposition of high-purity, Ge-rich crystalline and stoichiometric $Si_{0.50}Ge_{0.50}$ films on Si(100) using a new designer class of highly reactive, selectively chlorinated silylgermane compounds, such as ClH_2SiGeH_3 and $Cl_2HSiGeH_3$. Here we extend the synthetic "palette" of chlorinated Si−Ge analogs to the Ge-rich propane- and butane-like family of molecules including $SiH_2(GeH_3)_2$, $SiH(GeH_3)_3$, and $(SiH_2)_2(GeH_3)_2$. Our approach involves the controlled and selective chlorination of the $-SiH_2$, $-SiH$, and $-SiH_2-SiH_2-$ bridging ligands and leads to the pure compounds $ClHSi(GeH_3)_2$ (**1**), $Cl_2Si(GeH_3)_2$ (**2**), $ClSi(GeH_3)_3$ (**3**), and $ClHSiSiH_2(GeH_3)_2$ (**4**) in practical yields. The dichlorinated butane-like species $(ClHSi)_2(GeH_3)_2$ and $Cl_2SiSiH_2(GeH_3)_2$ are also obtained as isomeric mixtures. Here the availability of two equivalent Si sites has allowed us to investigate the order and degree of chlorination and establish that full substitution is preferred. All compounds were characterized by NMR, FTIR, and mass spectroscopy. First-principles density functional theory is used to elucidate the structural and vibrational trends of compounds **1**−**4** as well as a range of isomers of the dichlorinated butane-like derivatives. The observed FTIR frequencies and intensities of compounds **1**−**4** are accurately reproduced using the B3LYP/6-311N++G(3df,3pd) model chemistry, thus confirming the molecular structures, and our simulations are then used to obtain reliable vibrational mode assignments. Finally, we used $Cl_2Si(GeH_3)_2$ (**2**) to selectively grow silicon−germanium alloy semiconductors in the "source" and "drain" regions of simple transistor structures at 420 °C. XTEM imaging indicates commensurate growth of this material on the Si platform of the device. Experiments involving the more reactive $ClHSi(GeH_3)_2$ (**1**) analog produced $Si_{0.33}Ge_{0.67}$ layers with novel epitaxy-stabilized tetragonal structures exhibiting unprecedented compressive strain approaching −2.4%. This is ∼90% of the maximum value (2.75%) expected for this composition, and it is obtained in film thicknesses of 20−25 nm that far exceed the equilibrium critical value of the same material grown pseudomorphically on Si(100). The external stress required to achieve this deformation in free-standing samples is ∼4 GPa, which underscores the extreme strain state achieved in our films. This type of single-source deposition completely circumvents the need for the usual multicomponent reactions and corrosive Cl_2 etchants necessary to promote selective, strained-layer deposition in conventional processes.

Introduction

Germyl silanes are a family of deposition precursors with the general formula $SiH_{4-x}(H_3Ge)_x$ ($x = 1-4$), suitable for growth of thin $Si_{1-x}Ge_x$ films with a wide range of Ge contents at low temperatures under processing conditions inaccessible with currently available chemical precursors, notably germane gas and silanes.[1] $Si_{1-x}Ge_x$ alloys are utilized in vital components of computer chips, solar cells, and other semiconductor devices. In the case of logic chips, the materials already play a critical role in strained silicon technologies, enabling the continued pursuit of Moore's law for performance improvements. The $SiH_{4-x}(H_3Ge)_x$ compounds were recently synthesized and have been subsequently used to fabricate $Si_{1-x}Ge_x$ alloys advantageously.[2] This work in turn led to the discovery of new branches within the general silyl−germyl class including butane-like analogs and chlorinated derivatives of SiH_3GeH_3 including the $Cl_2HSiGeH_3$ and ClH_2SiGeH_3 compounds.[3,4] The high reactivity and built-in Cl functionalities were designed to facilitate selective growth compatible with low-temperature CMOS processing. Epitaxy of these compounds at 380−430 °C produces stoichiometric $Si_{0.50}Ge_{0.50}$ films seamlessly, conformally, and selectively in the "source/drain" regions of prototypical device structures.[5] In this case, and in general, the chlorine-containing deposition byproducts function as in situ etchants which preferentially remove amorphous material

* To whom correspondence should be addressed.

(1) Ritter, C. J.; Hu, C.; Chizmeshya, A. V. G.; Tolle, J.; Klewer, D.; Tsong, I. S. T.; Kouvetakis, J. *J. Am. Chem. Soc.* **2005**, *127* (27), 9855.

(2) Hu, C.-W.; Menendez, J.; Tsong, I. S. T.; Tolle, J.; Chizmeshya, A. V. G.; Ritter, C.; Kouvetakis, J. *Appl. Phys. Lett.* **2005**, *87* (18), 181903.

(3) Chizmeshya, A. V. G.; Ritter, C. J.; Hu, C.-W.; Tice, J. B.; Tolle, J.; Nieman, R.; Tsong, I. S. T.; Kouvetakis, J. *J. Am. Chem. Soc.* **2006**, *128* (21), 7950.

(4) Tice, J. B.; Chizmeshya, A. V. G.; Roucka, R.; Tolle, J.; Cherry, B. R.; Kouvetakis, J. *J. Am. Chem. Soc.* **2007**, *129* (25), 6919.

(5) Fang, Y.-Y.; Tice, J. B.; Chizmeshya, A. V. G.; Tolle, J.; D'Costa, V. R.; Menendez, J.; Kouvetakis, J. *Appl. Phys. Lett.*, submitted for publication.

10.1021/cm800427p CCC: $40.75
Published on Web 06/11/2008

from unmasked regions at a much higher rate than its crystalline counterpart grown on exposed Si surfaces, thus promoting selective growth of a variety of device structures on patterned Si wafers.[6] The materials deposited via this method exhibit exceptional morphological and structural properties including high compressive strains. The latter can dramatically increase the hole mobility in conventional transistors, resulting in a concomitant improvement of the device operating speed.[7,8]

Typically the strain states needed for this application are obtained by selective epitaxy of $Si_{1-x}Ge_x$ alloys which are deposited on unmasked Si as perfectly pseudomorphic films within the source (S) and drain (D) areas of individual transistors. The larger lattice spacing of the alloy in the S/D regions induces a tetragonal compressive strain on the adjacent active Si areas (including the channel) with a magnitude that is proportional to the Ge concentration. To date, Ge concentrations of ∼20−30% can routinely be achieved in commercial processes leading to a ∼20% increase in the saturation current of a typical state-of-the-art device.[9,10] This implies that any further improvements in carrier mobility will require higher Ge concentrations to achieve the unprecedented compressive strains associated with the larger $Si_{1-x}Ge_x$/Si lattice mismatches within the device structure. This will lead to significant performance gains in next-generation devices compared to the current 30% Ge stressor limit.

Conventional, high-temperature selective growth of $Si_{1-x}Ge_x$ alloys using reactions of chlorosilanes, germane, and elemental Cl_2 becomes problematic particularly as the Ge content in the alloy increases beyond the current state-of-the art limit of 30%. Typically the materials produced exhibit high threading dislocation densities and nonuniformities in strain and thickness which ultimately can degrade the quality and performance of the stressor, thereby limiting its practical usefulness. The extreme processing conditions also vitiate compositional control and promote significant intermixing at the various interfaces, making pseudomorphic growth of uniformly strained films increasingly difficult to achieve as the Ge concentration is increased beyond 30 atom %.[11]

The focal point of our present studies is therefore to produce new classes of chlorinated Si−Ge precursors and assess their applicability in low-temperature selective-area deposition processes. A unique advantage of our chlorinated precursor-based approach is that the Si−Ge molecular cores are incorporated intact into the films, thereby providing

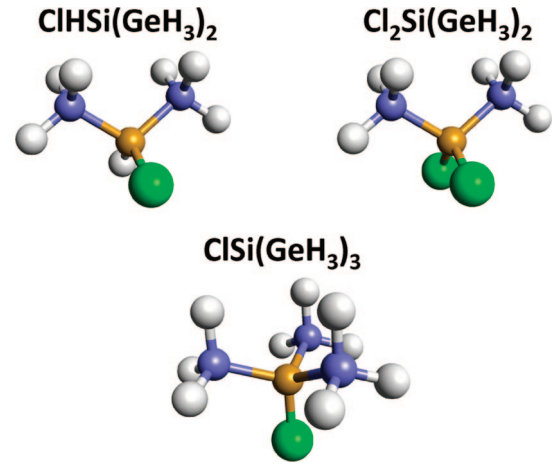

Figure 1. Structural representations of the $ClHSi(GeH_3)_2$ (**1**), $Cl_2Si(GeH_3)_2$ (**2**), and $ClSi(GeH_3)_3$ (**3**) molecules. A detailed theoretical treatment of these structures is described in a subsequent section.

precise control of composition. In addition, these compounds are expected to function as built-in cleaning agents during in situ selective growth of a variety of device structures on patterned Si wafers. For the previously mentioned ClH_2SiGeH_3 and $Cl_2HSiGeH_3$ compounds the built-in SiGe composition and high reactivity provide precise control with regard to complete HCl elimination and simultaneously enable incorporation of the desired $Si_{0.50}Ge_{0.50}$ content in the purest possible form.

While the composition in this case is limited to 50 atom %, a further increase in strain will require higher Ge contents which can, in principle, then be obtained by use of heavier chlorinated derivatives such as $ClHSi(GeH_3)_2$ (**1**), $Cl_2Si(GeH_3)_2$ (**2**), and $ClSi(GeH_3)_3$ (**3**). These compounds could function as etching agents for removal of amorphous material at even lower temperatures during in situ selective growth. In addition, their higher masses would limit their desorption from the growth front by enhancing their sticking behavior, thereby providing an additional tuning mechanism for effective selectivity under a wider range of processing conditions. This approach therefore provides a new paradigm for precursor-driven stress engineering which could lead to significant performance gains in silicon-based microelectronics.

In this paper we describe the preparation and properties of chlorinated $H_2Si(GeH_3)_2$ and $HSi(GeH_3)_3$ to complete the entire genus of $SiH_{4-x}(H_3Ge)_x$ compounds containing Si−Cl bonds (Figure 1). The synthetic method is expanded to include Si-selective chlorination of butane-like analogs such as the $(SiH_2)_2(GeH_3)_2$ macromolecular hydride to produce the $ClHSiSiH_2(GeH_3)_2$ (**4**) and $Cl_2SiSiH_2(GeH_3)_2$ derivatives. The structural, vibrational, and thermochemical properties for all of these compounds are explored in detail using state-of-the-art simulation techniques. Finally, we conducted proof-of-principle experiments in both selective-area deposition and strained layer epitaxy of $Si_{1-x}Ge_x$ alloys using the newly prepared compounds. Together these experiments demonstrate that the chlorinated compounds are viable CVD sources for applications in microelectronic device processing requiring high compressive strain and straightforward low-temperature selective formation of highly homogeneous com-

(6) Kiyota, Y.; Udo, T.; Hashimoto, T.; Kodama, A.; Shimamoto, H.; Hayami, R.; Ohue, E.; Washio, K. *IEEE Trans. Electron Devices* **2002**, *49* (5), 739–745.
(7) (a) Ghani, T.; Armstrong, M.; Auth, C.; Bost, M.; Charvat, P.; Glass, G.; Hoffmann, T.; Johnson, K.; Kenyon, C.; Klaus, J.; McIntyre, B.; Mistry, K.; Murthy, A.; Sandford, J.; Silberstein, M.; Sivakumar, S.; Smith, P.; Zawadzki, K.; Thompson, S.; Bohr, M. *IEDM Technol. Dig.* **2003**, 1161.
(8) Wang, G. H.; Toh, E.-H.; Tung, C.-H.; Du, A.; Lo, G.-Q.; Samudra, G.; Yeo, Y.-C. *Jpn. J. Appl. Phys.* **2007**, *46* (4B), 2062–2066.
(9) Ang, K.-W.; Chui, K.-J.; Bliznetsov, V.; Tung, C.-H.; Du, A.; Balasubramanian, N.; Samudra, G.; Fu Li, M.; Yeo, Y.-C. *Appl. Phys. Lett.* **2005**, *86*, 93102.
(10) Ang, K.-W.; Tung, C.-H.; Balasubramanian, N.; Samudra, G. S.; Yeo, Y.-C. *IEEE Electron Devices Lett.* **2003**, *28* (7), 609.
(11) Bogumilowicz, Y.; Hartmann, J. M.; Fabri, J. M.; Billon, T. *Semicond. Sci. Technol.* **2006**, *21*, 1668–1674.

positions in the "source/drain" regions of prototypical transistors. The single-source approach involving highly reactive species represents a significant advantage over the conventional multistep routes.

Results and Discussion

In our previous studies, the chlorination of H_3SiGeH_3 was readily obtained by reactions with BCl_3 to produce ClH_2SiGeH_3 and $Cl_2HSiGeH_3$ and polysubstituted derivatives according to the equation $n BCl_3 + 3H_3SiGeH_3 \rightarrow (n/2)B_2H_6 + 3Cl_nH_{6-n}SiGe$.[4] This scheme represents a viable single-step route to the target compounds in practical yields for industrial-level semiconductor applications, particularly once the starting SiH_3GeH_3 material is produced on a commercial scale by Voltaix. Higher order polychlorinated derivatives such as $Cl_2SiHGeH_2Cl$, $Cl_2SiHGeHCl_2$, $ClSiH_2GeH_2Cl$, and $ClSiH_2GeHCl_2$ represent a new class of highly reactive compounds that are of fundamental and practical interest for generating Ge-rich semiconductor alloys. In the present work preparation of the $ClHSi(GeH_3)_2$ (**1**), $Cl_2Si(GeH_3)_2$ (**2**), and $ClSi(GeH_3)_3$ (**3**) analogs was also conducted via selectively controlled chlorination of the Si site using reactions of BCl_3 with the corresponding hydrides in the absence of solvents. The $SiH_2(GeH_3)_2$ and $SiH(GeH_3)_3$ starting materials were synthesized and characterized via procedures developed in a previous investigation.[1]

A. Synthetic Routes to $ClHSi(GeH_3)_2$ (1) and $Cl_2Si(GeH_3)_2$ (2). The monochlorinated species **1** was generated by direct combination of BCl_3 and $SiH_2(GeH_3)_2$ in a 1:3 molar proportion via evolution of diborane according to eq 1

$$BCl_3 + 3SiH_2(GeH_3)_2 \rightarrow 0.5B_2H_6 + 3ClHSi(GeH_3)_2 \quad (1)$$

The target compound (**1**) was isolated by trap-to-trap fractionation as a colorless, pyrophoric liquid with a room-temperature vapor pressure of ~14 Torr. A typical reaction was allowed to proceed at 0 °C for 2 h and produced pure single-phase material in significant yields (~40%) based on the amount of the starting hydride material used. The latter was recovered under these optimum conditions and recycled in subsequent preparations. Attempts to increase the yield by extending the reaction time generated mixtures of monochloro compound **1** with minor amounts of the disubstituted derivative $Cl_2Si(GeH_3)_2$ (**2**). To enhance formation of **2** we increased the Cl activity in the reaction medium using higher molar ratios of BCl_3 and $SiH_2(GeH_3)_2$. For a stoichiometric 2:3 combination of the reactants as described by eq 2 we obtained a mixture of **1** and **2** in yields of 20% and 15%, respectively, indicating a significant increase of the second chlorination at the Si center, as expected.

$$2BCl_3 + 3SiH_2(GeH_3)_2 \rightarrow B_2H_6 + 3Cl_2Si(GeH_3)_2 \quad (2)$$

When the chlorine activity was further increased by combining the reactants in ~1:1 molar ratio the $Cl_2Si(GeH_3)_2$ (**2**) species was predominately produced (20% yield) while formation of $ClHSi(GeH_3)_2$ (**1**) was essentially suppressed (1% yield). In both cases copious amounts of diborane byproducts were evolved in addition to a polymeric solid, which was present in quantities insufficient for a reliable characterization. Pure compound **2** was then isolated as a volatile colorless liquid by trap-to-trap distillation (vapor pressure of 7 Torr at 22 °C).

Table 1. ^{1}H and ^{29}Si Shifts and Si−H and H−H *J* Coupling Constants (Hz) for the $Cl_nH_{4-n-m}Si(GeH_3)_m$ (m = 2 and 3) Species[a]

compound	δ^1H(SiH_x)	δ^1H(GeH_x)	δ^{29}Si	$^1J_{Si-H}$	$^2J_{Si-H}$	$^3J_{H-H}$
$SiH_2(GeH_3)_2$	3.39 (sept)	3.11 (t)	−102.7	200.3		3.9
$ClHSi(GeH_3)_2$	5.07 (sept)	3.28 (d)	−14.7	223.3	14.7	3.5
$Cl_2Si(GeH_3)_2$		3.42 (s)	30.2		13.0	
$HSi(GeH_3)_3$	3.35 (dt)	3.26 (d)	−112.8			3.4
$ClSi(GeH_3)_3$		3.49 (s)	−8.1		10.3	

[a] All compounds were dissolved in C_6D_6 and referenced to TMS.

B. Synthetic Routes to $ClSi(GeH_3)_3$ (3). Preparation of compound **3** was initially explored by stoichiometric 3:1 combinations of $SiH(GeH_3)_3$ and BCl_3. These typically produced mixtures of the $ClSi(GeH_3)_3$ and $SiH(GeH_3)_3$ compounds which were impossible to separate due to the similarity in their boiling points. Prolonged reaction times eventually led to formation of nonvolatile polymeric solids which are likely derived from decomposition of polychlorinated trigermylsilanes. This indicates that over time chlorination occurs at the Ge sites in addition to Si eventually producing unstable products. However, preparation of compound **3** was readily obtained in ~20% yield at 0 °C and a 10 min reaction time using a 1:1 molar ratio of $SiH(GeH_3)_3$ and BCl_3. Pure compound **3** is a stable, colorless liquid with a room-temperature vapor pressure of ~2 Torr.

C. Structural Characterization by NMR. Due to their high reactivity compounds **1**, **2**, and **3** were predominately characterized by physical methods rather than conventional elemental analyses. In particular, their compositions were determined and structures elucidated by extensive ^{1}H and ^{29}Si nuclear magnetic resonance (NMR) analyses such as ^{1}H correlated spectroscopy (COSY) and ^{1}H−^{29}Si HMQC techniques. These data were further corroborated by mass spectrometry and gas-phase FTIR measurements. Collectively, the spectroscopic results combined with DFT theoretical simulations of the IR spectra unequivocally confirm the proposed molecular structures shown in Figure 1.

Table 1 lists the ^{1}H and ^{29}Si chemical shifts as well as the J_{Si-H} and J_{H-H} coupling constant values derived from our measurements for the chlorinated compounds including the corresponding pure hydride reactants. These chemical shifts in combination with the coupling constants are particularly useful because they unambiguously establish the connectivities of the H and Cl atoms to the Si−Ge molecular core for each compound in the various products. The ^{29}Si satellite peaks exhibit $^1J_{Si-H}$ and $^2J_{Si-H}$ coupling constants with nominal values in the expected range of 200−230 and 10−15 Hz, respectively. The $^3J_{H-H}$ values also span the typical range of 3−4 Hz. We note that for compound **1** the $^1J_{Si-H}$ value increases with increasing number of Si−Cl bonds, while the opposite is observed for the $^3J_{H-H}$ values. The identical trend was found in our chlorination studies of the SiH_3GeH_3 species.

The ^{1}H NMR spectra show the expected multiplicity in various SiH_x and GeH_x peaks, and the ^{29}Si resonances are perfectly consistent with the presence of Si−Cl bonds. The ^{1}H spectra of **1** showed the GeH_3 resonance as a doublet at

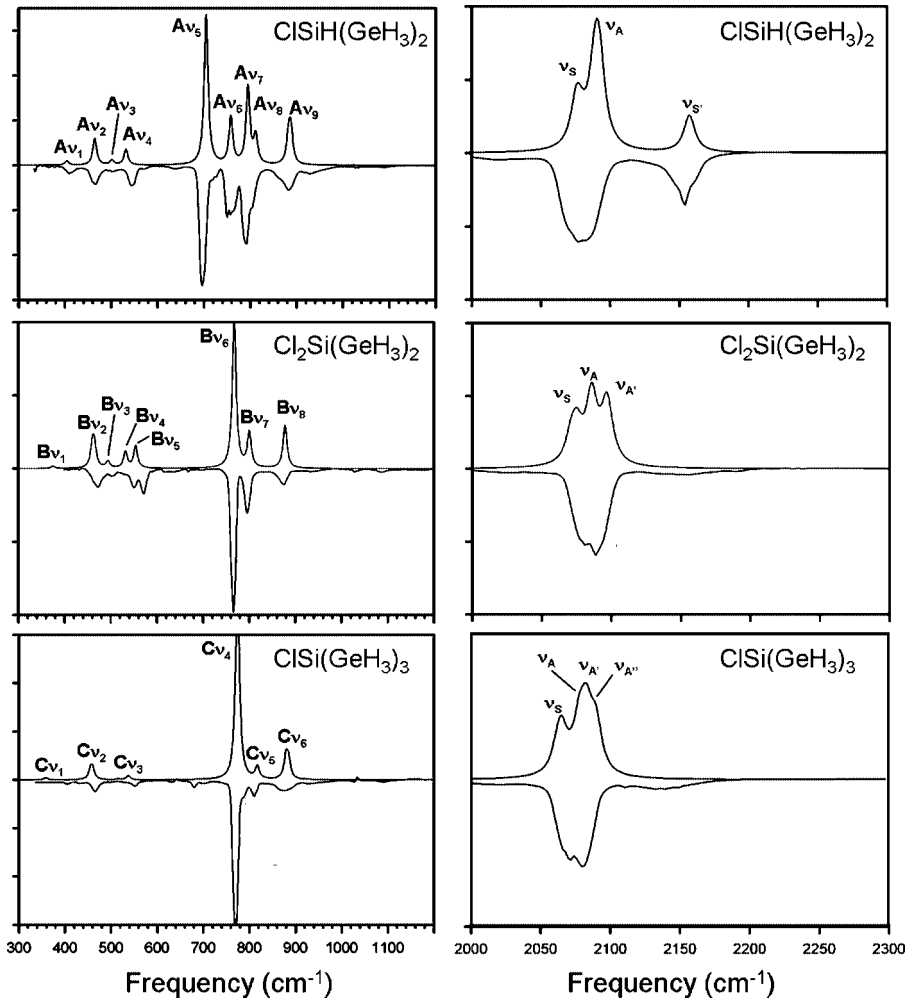

Figure 2. Comparisons of the calculated (top) and observed (bottom) room-temperature IR spectra of molecules **1**, **2**, and **3**. Frequency scale factors of 0.989 and 0.979 were applied to the calculated low- and high-frequency spectra, shown in the left and right panels, respectively. The labels attached to the various spectral features are described in Table 2.

3.28 ppm and the SiH resonance as a septet centered at 5.07 ppm. These are shifted downfield with respect to GeH_3 (3.11 ppm) and SiH_2 (3.39 ppm) of the starting $SiH_2(GeH_3)_3$ material, consistent with substitution of H on the Si atom by the electron-withdrawing Cl atom. The $^1H-^{29}Si$ HMQC spectrum also determined that the proton at 5.07 ppm is bound to a Si atom at −14.7 ppm. The integrated SiH/GeH_3 peak intensity ratio is 1:6, as expected. The GeH_3 resonance of **2** was observed as a singlet at 3.42 ppm, representing a further downshift compared to compound **1**, consistent with a second substitution of Cl on the Si. The ^{29}Si peak is observed at 30.2 ppm, which is significantly shifted downfield compared to those of $SiH_2(GeH_3)_3$ (δ −102.7) and $ClHSi(GeH_3)_2$ (δ −14.7). Almost identical trends were observed in the NMR spectra of the trigermyl compound **3**, for which chlorination of the single Si−H site leads to a slight downfield shift of the GeH_3 peak with respect to the pure hydride. Similarly, chlorination of the Si site leads to an ∼100 ppm shift of the corresponding ^{29}Si peak.

It is interesting to point out that the same general trends were exhibited by the simpler silylgermane series where the ^{29}Si peaks of the SiH_3GeH_3, $ClSiH_2GeH_3$, and $Cl_2SiHGeH_3$ were observed at −91.6, −24.6, and + 9.8 ppm, respectively. Here the net shift upon dichlorination of the Si site is also ∼100 ppm, and this appears to be generally true for the full chlorination digermyl and trigermyl compounds described here.

The mass spectra of the compounds were obtained by direct insertion and revealed peaks corresponding to the corresponding molecular ions. Their fragmentation patterns were consistent with the proposed molecular structures for $ClHSi(GeH_3)_2$ (**1**), $Cl_2Si(GeH_3)_2$ (**2**), and $ClSi(GeH_3)_3$ (**3**). Their IR spectra were obtained from measurements on gaseous samples, and the data were compared to those derived from a complete first-principles analysis of the vibrational properties as described in detail below.

D. Vibrational Properties of $ClHSi(GeH_3)_2$ (1), $Cl_2Si(GeH_3)_2$ (2), and $ClSi(GeH_3)_3$ (3). The IR spectra of these molecules were simulated using the same approach used in our previous work on related germylsilanes and butane-like analogs (the computational procedures are described in detail below). The normal modes exhibited positive definite vibrational frequencies, indicating that the ground-state structures are dynamically stable. Symmetry analysis of the optimized structures indicates that molecules **1**, **2**, and **3** adopt point groups of C_s, C_{2v}, and C_{3v}, respectively. A detailed comparison of the calculated and observed spectra is presented in Figure 2, and the various peak assignments

Table 2. Harmonic Vibrational Frequencies of the $ClHSi(GeH_3)_2$ (1), $Cl_2Si(GeH_3)_2$ (2), and $ClSi(GeH_3)_3$ (3) Molecules and Their Corresponding Assignments[a]

$ClHSi(GeH_3)_2$		$Cl_2Si(GeH_3)_2$		$ClSi(GeH_3)_3$	
$A_{v1}(400)$	a GeH_3 + SiH wag	$B_{v1}(371)$	a GeH wag	$C_{v1}(355)$	a GeH wag
$A_{v2}(459)$	s GeH_3 + SiH wag	$B_{v2}(456)$	a GeH_3 wag	$C_{v2}(451)$	independent GeH_3 wags
		$B_{v2'}(460)$	s GeH_3 wag	$C_{v2'}(453)$	
				$C_{v2''}(455)$	
$A_{v3}(497)$	s GeH_2 wag	$B_{v3}(489)$	a GeH wag		
$A_{v4}(526)$	Si−Cl str	**$B_{v4}(526)$**	s Si−Cl_2 **str**	**$C_{v3}(531)$**	Si−Cl str
		$B_{v5}(548)$	a Si−Cl_2 **str**		
$A_{v5}(689)$	s SiH wag				
$A_{v6}(750)$	SiH rock				
$A_{v7}(786)$	a GeH rock	$B_{v6}(760)$	a GeH_3 rock	$C_{v4}(767)$	GeH_3 rock
$A_{v8}(803)$	s GeH_3 rock	$B_{v7}(791)$	s GeH_3 rock	$C_{v5}(808)$	s GeH_3 rock
$A_{v9}(878)$	s GeH wag + GeH_2 scis	$B_{v8}(878)$	s GeH wag + s GeH_2 scis	$C_{v6}(874)$	s GeH wag + s GeH_2 scis
$v_S(2074)$	s GeH_3 str	$v_S(2072)$	s GeH_3 str	v_S (2067)	s GeH_3 str
$v_A(2089)$	a GeH_3 str	v_A (2083)	a GeH_2 str	v_A (2079)	s GeH str
$v_{S'}(2153)$	SiH str	$v_{A'}(2095)$	a GeH str	$v_{A'}(2084)$	a GeH_2 str
				$v_{A''}(2092)$	a GeH str

[a] Scale factors of 0.989 and 0.979 have been applied to the calculated low-frequency (<1000 cm^{-1}) and high-frequency (>2000 cm^{-1}) data, respectively. Here s and a denote symmetric and asymmetric, while str and scis denote stretching and scissor motion.

obtained from a normal-mode analysis are listed in Table 2. The data in general indicate that there is a close match between theory and experiment. The experimental spectra of $ClHSi(GeH_3)_2$ (**1**) show a weak band at 2150 cm^{-1} corresponding to the stretching mode of the single Si−H bond in the molecule. The corresponding theoretical value is calculated to occur at 2153 cm^{-1}. The spectra of $Cl_2Si(GeH_3)_2$ (**2**) and $ClSi(GeH_3)_3$ (**3**) do not contain Si−H stretching bands, as expected. All of the simulated high-frequency spectra contain the symmetric GeH_3 stretching band with an average frequency of 2072 cm^{-1}, while the average experimental value is virtually the same at 2080 cm^{-1}. For example, the asymmetric GeH_3 stretching band for **1** is obtained as a single peak (2085 cm^{-1}), while the corresponding bands for **2** and **3** appear to be split about this value by about ∼10−15 cm^{-1} into a doublet and triplet, respectively. This is in reasonable agreement with the experimental splittings which are measured to be about 10 cm^{-1}, around the average central value in the range of 2085−2100 cm^{-1}. Although the theoretical and experimental spectra exhibit the same peak multiplicity there slight differences in the absolute frequencies, and these appear to be consistent with our prior comparisons for Si−Ge hydrides using the same approach.[4]

The simulated low-frequency spectra (200−1200 cm^{-1}) are significantly more complex, and the mode assignments for these are also given in Table 2. As can be seen from Figure 2, the close agreement found between experiment and theory suggests that the mode assignments listed in the table are reliable. According to our analysis, the most intense band in the Si−H-containing $ClHSi(GeH_3)_2$ (**1**) compound occurs at ∼692 cm^{-1} and corresponds to the "classic" wagging motion of this bond. In the two other Si perchlorinated compounds **2** and **3** the strongest bands occur near ∼762 cm^{-1} and correspond to the asymmetrical GeH_3 rocking vibrations. The spectra of all three compounds contain Si−Cl stretches in the range 524−554 cm^{-1}. The symmetry splitting of this band is only observed in the dichlorinated species $Cl_2Si(GeH_3)_2$ (**2**), as expected. Additional assignments consistent with the proposed structures, by frequency range, are as follows: (i) 356−405 cm^{-1}, GeH and SiH wagging vibrations; (ii) 455−465 cm^{-1}, GeH_3 wagging vibrations; (iii) 791−811 cm^{-1}, symmetric GeH_3 rocking vibrations; (iv) ∼877 cm^{-1}, symmetric GeH wagging and GeH_2 scissor vibrations.

We note that in the above vibrational analysis the scale factors of 0.989 and 0.979 were found to produce an optimal match for the low- and high-frequency spectra, respectively. These are nearly identical to the values used to analyze numerous other Si−Ge hydride macromolecules and their halogenated derivatives,[1,3,4,12] indicating the broad applicability and reliability of these numerical factors in describing this class of compounds.

E. Chlorination of Bridging Si Sites in Butane-Like $(SiH_2)_2(GeH_3)_2$. The chlorination studies of $SiH_{4-x}(H_3Ge)_x$ hydrides have shown that the Si site is preferentially chlorinated to produce a range of new compounds. However, in the case of the simplest SiH_3GeH_3 species this prior work established that consecutive chlorinations of terminal Si−H bonds are difficult to achieve. On the other hand, chlorination of propane-like molecules containing bridging SiH_2 single centers such as $SiH_2(GeH_3)_2$ is much more straightforward. This is also found to be the case for the isostructural trisilane $SiH_2(SiH_3)_2$,[13] where its bridging SiH_2 is the most susceptible site to full chlorination while the terminal Si−H bonds are significantly less prone to this type of substitution. In view of this reaction behavior, we pursued a brief study to explore chlorination of related Si−Ge-based macromolecules that offer a greater capacity for Si−H substitutions at bridging sites. These compounds are designed not to contain terminal Si−H bonds but rather incorporate highly reactive $-SiH_2-SiH_2-$ linkages exclusively. The simplest candidate that fulfills these criteria is the butane-like $(SiH_2)_2(GeH_3)_2$ species which we previously prepared and studied in detail from a fundamental and practical perspective. The availability of two equivalent reaction sites in this molecule makes the order and degree of chlorination of fundamental interest and represents a natural extension of our synthetic strategy to

(12) Chizmeshya, A. V. G.; Ritter, C.; Tolle, J.; Cook, C.; Menendez, J.; Kouvetakis, J. *Chem. Mater.* **2006**, *18* (26), 6266–6277.
(13) Drake, J. E.; Goddard, N. *Inorg. Nucl. Chem. Lett.* **1968**, *4* (7), 385–8.

produce an entire genus of halogenated Si−Ge macromolecular hydride derivatives containing SiGe, GeSiGe, and GeSiSiGe cores. Finally, in view of our success in reconciling simulated structural and spectroscopic properties with experiment for the simpler members of this family we undertook a systematic study of the entire sequence of $Cl_nH_{4-n}Si_2(GeH_3)_2$ ($n = 1-4$) molecules and all possible conformations to explore the reaction trends in this more complex system.

F. Synthesis and Characterization of $ClHSiSiH_2(GeH_3)_2$ (4) and $Cl_2H_2Si_2(GeH_3)_2$. The monosubstituted $ClHSiSiH_2(GeH_3)_2$ (**4**) species was readily obtained by reacting an excess of BCl_3 with $(SiH_2)_2(GeH_3)_2$ in a 2:3 ratio. A typical reaction time of 1 h at an optimum temperature of 0 °C yielded diborane, but also a small amount of unreacted starting material was recovered under these conditions as confirmed by NMR. Efforts to achieved full conversion of $(SiH_2)_2(GeH_3)_2$ using longer reaction times and higher temperatures produced intractable polymeric solids that could not be fully characterized. Compound **4** was isolated by distillation as a colorless liquid with a nominal vapor pressure of ~2 Torr. Its ^{29}Si spectrum showed two peaks due to the SiH_2 and SiHCl moieties at −97.0 and −15.0 ppm, respectively. These are downshifted with respect to the SiH_2 resonance (δ −105.0) of the starting material and consistent with a single chlorine substitution at the Si center. The ^1H spectra revealed a triplet (δ 3.05), pentet (δ 3.33), sextet (δ 5.02), and doublet (δ 3.26) corresponding to protons bonded in the sequence of $GeH_3-SiH_2-SiHCl-GeH_3$. The integrated intensities, coupling patterns, and positions of the peaks collectively point to this atomic arrangement. The shift corresponding to the Ge−H furthest from the Cl site (δ 3.05) is close to that of the starting material (δ 3.11), while the shift of the Ge−H adjacent to the SiHCl is slightly downshifted (δ 3.26). The SiH_2 peak (δ 3.33) is remarkably close to that of the starting material (δ 3.29) and to other bridging SiH_2 ligands in silylgermane compounds. The sextet corresponding to the SiHCl (δ 5.02) is significantly downshifted due to the presence of Cl and close to the one observed in $ClHSi(GeH_3)_2$ (δ 5.07). The molecular structure is further confirmed with 2D ^1H COSY, which yielded the following correlations: (i) The 3.26 (doublet) and the 5.02 (sextet) are associated with $-GeH_3-SiHCl-$, (ii) the 5.02 (sextet) and 3.33 (pentet) are associated with $-SiHCl-SiH_2-$, and (iii) the 3.33 (pentet) and 3.05 (triplet) are associated with $-SiH_2-GeH_3-$. The $^1H-^{29}Si$ HMQC NMR corroborated the latter assignments and indicated direct couplings between the ^{29}Si (δ −97) and the ^1H (3.33, pentet) and between the ^{29}Si (δ −15) and the ^1H (δ 5.02, sextet).

The compound was also characterized by IR, and the spectrum was in perfect agreement with the theoretical counterpart as shown in Figure 3. To be consistent with the calculations of $ClSiH(GeH_3)_2$ (**1**), $Cl_2Si(GeH_3)_2$ (**2**), and $ClSi(GeH_3)_3$ (**3**) described above we employed the same frequency scale factors for this compound. A complete vibrational analysis for the 11 dominant features in the low-frequency spectrum yields the following assignments (also listed in Table 3): (i) an SiH_2 rocking mode D_{v1} at 339 cm^{-1}, (ii) D_{v2}, D_{v3}, various symmetric GeH_2, GeH_3, and SiH wagging vibrations, (iii) Si−Cl stretching vibrations at 522 cm^{-1}, assigned as D_{v4}, (iv) Si−H rocking (D_{v5}, D_{v6}) and wagging modes (D_{v7}, D_{v8}) 640−770 cm^{-1} range, (v) asymmetrical GeH_3 rocking vibrations (D_{v9}) at 785 cm^{-1}, and (vi) GeH_2 (D_{v10}) and SiH_2 (D_{v11}) scissor-like vibrations transverse to the molecular backbone. The Ge−H and Si−H stretching bands in the 2000−2200 cm^{-1} range exhibit complex structure associated with the presence of the Cl atom, which prohibits synchronous GeH_3 group vibrations at both ends of the molecule. Instead, the GeH_3 and SiH_2/SiH moieties vibrate independently at slightly different frequencies. Accordingly, the symmetric GeH_3 stretches are observed as two bands (ν_S and $\nu_{S'}$) near 2070 cm^{-1}, while

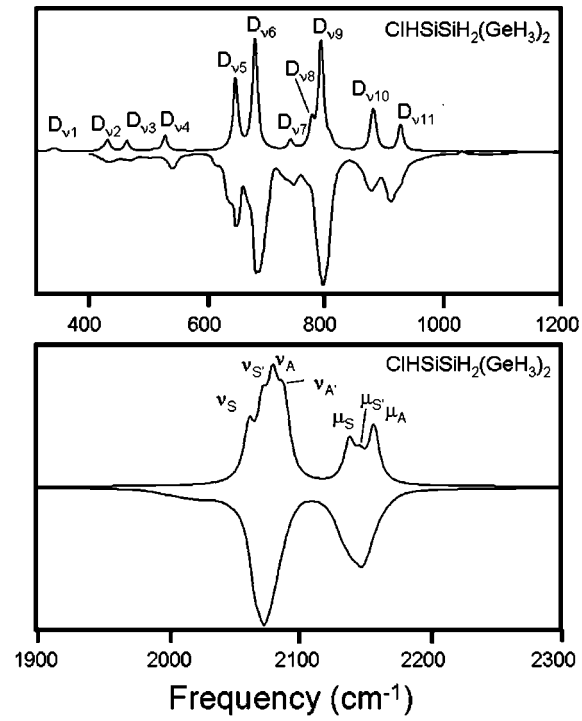

Figure 3. Calculated and observed room-temperature IR spectra of the pure monochlorinated $ClHSiSiH_2(GeH_3)_2$ molecule. Frequency scale factors of 0.989 and 0.979 were applied to the calculated low- and high-frequency spectra, shown in the top and bottom panels, respectively. The labels attached to the various spectral features are described in Table 3.

Table 3. Harmonic Vibrational Frequencies of the $ClHSiSiH_2(GeH_3)_2$[a]

D_{v1}(339)	SiH_2 rock ⊥ core
D_{v2}(425)	s GeH_3 + SiH wag
D_{v3}(458)	s GeH_2 wag
D_{v4}(522)	Si−Cl str
D_{v5}(642)	a Si−H wag
D_{v6}(675)	s Si−H wag
D_{v7}(734)	a Si−H rock
D_{v8}(769)	s Si−H rock
D_{v9}(785)	a GeH_3 rock
D_{v10}(875)	s GeH wag + s GeH_2 scis
D_{v11}(919)	SiH_2 scis
ν_S(2064)	s GeH_3 str
$\nu_{S'}$(2075)	s GeH_3 str
ν_A(2083)	a GeH_3 str
$\nu_{A'}$(2092)	a GeH_3 str
μ_S(2141)	s SiH_2 str
$\mu_{S'}$(2149)	s SiH_2 str
μ_A(2160)	a SiH_2 str

[a] Scale factors of 0.989 and 0.979 have been applied to the calculated low-frequency (<1000 cm^{-1}) and high-frequency (>2000 cm^{-1}) data, respectively. Here s and a denote symmetric and asymmetric, while str and scis denote stretching and scissor motion.

the corresponding asymmetric stretches (ν_A and $\nu_{A'}$) occur around 2088 ± 5 cm^{-1}. A similar splitting occurs for the symmetric Si−H stretches (denoted by μ_S and $\mu_{S'}$), while the corresponding asymmetrical vibration, μ_A, is found at 2160 cm^{-1}.

The dichlorinated $Cl_2H_2Si_2(GeH_3)_2$ species was obtained as a mixture of two substitutional isomers, $Cl_2SiSiH_2(GeH_3)_2$ and $(ClHSi)_2(H_3Ge)_2$. Liquid samples with a vapor pressure of ∼1 Torr were prepared by reactions of BCl_3 and $(SiH_2)_2(GeH_3)_2$ in a 1:1 ratio at 0 °C. The reaction time in this case was considerably reduced to ∼20 min compared to the monochlorination to avoid formation or mitigate decomposition of unstable byproducts that were also produced under these conditions. Additional substitution of more than two Cl atoms was extensively investigated, but all of these experiments inevitably led to breakdown of the Ge−Si−Si−Ge framework, resulting in formation of polymeric materials rather than the desired molecules. Therefore, further attempts to multiply chlorinate $(SiH_2)_2(GeH_3)_2$ via this method were not pursued.

The very close boiling points of the dichlorinated $Cl_2SiSiH_2(GeH_3)_2$ and $(ClHSi)_2(H_3Ge)_2$ derivatives precluded their individual separation by normal distillation or fractionation techniques. Accordingly, their identity was established, and their structures were primarily elucidated by ^1H and ^{29}Si NMR including 2D ^1H COSY and $^1H-^{29}Si$ HMQC analyses. For the $(ClHSi)_2(H_3Ge)_2$ species the proton NMR spectra showed a doublet at 3.26 ppm due to the terminal GeH_3 protons and a pentet at 4.98 ppm corresponding to the bridging SiH protons. The integrated intensity ratio of the GeH_3 and SiH peaks were found to be 3:1, respectively, as expected. The ^1H spectra also displayed three additional peaks at 3.43 (singlet), 3.42 (quartet), and 3.07 (triplet) ppm, which were assigned to the GeH_3, SiH_2, and GeH_3 protons of the sequence contained in the $H_3Ge-SiCl_2-SiH_2-GeH_3$ species. The ^{29}Si spectra of the samples exhibited three distinct resonances at 24.4, −88.7, and −17.0 ppm corresponding to the $SiCl_2$ and SiH_2 of $H_3Ge-SiCl_2-SiH_2-GeH_3$ and SiH of $(ClHSi)_2(H_3Ge)_2$, respectively. Note that the SiH_2 ^{29}Si resonance of the $Cl_2SiSiH_2(GeH_3)_2$ is significantly shifted downfield (δ −88.7) with respect to the starting material (δ −105.0) due to the presence of the chlorine atoms bound to the adjacent silicon. The proposed structures of $(ClHSi)_2(H_3Ge)_2$ and $Cl_2SiSiH_2(GeH_3)_2$ are further confirmed by a 2D ^1H COSY spectrum, which only show two sets of cross peaks correlating to Ge−H and Si−H resonances at 3.26 and 4.98 ppm as well as 3.07 and 3.42 ppm, respectively. The $^1H-^{29}Si$ HMQC spectrum revealed that the protons at 4.98 and 3.42 ppm are directly coupled to ^{29}Si resonances at −17.0 and −88.7 ppm, respectively.

The compounds were also characterized by IR, and the spectrum of the mixture was in perfect agreement with the theoretical simulations. In previous investigations, we successfully used simulated vibrational spectra to identify the various positional and conformational isomers in a mixture of the pure hydride compounds $(SiH_2)_2(GeH_3)_2$ and $GeH_2SiH_2(GeH_3)_2$.[3] Accordingly, in the present study the vibrational spectra for the $Cl_2SiSiH_2(GeH_3)_2$ and $(ClHSi)_2(H_3Ge)_2$ mixture was modeled as a combination of the three possible positional species including the $Cl_2SiSiH_2(GeH_3)_2$ compound and two conformers of $(ClHSi)_2(H_3Ge)_2$ in which the Cl substitutions occur symmetrically or asymmetrically with respect to the plane of the Ge−Si−Si−Ge core. These three molecular structures and their labeling as Cl-2a, Cl-2b, and Cl-2c, respectively, are shown in the top panel of Figure 4. Also shown in the figure are the individual simulated spectra of these compounds together with that of the monochlorinated species which is labeled as Cl-1. Here we briefly describe the key trends, focusing first on the features common to all low-frequency spectra (300−1200 cm^{-1}). These are labeled 1−9 and correspond to the following vibrational assignments: (1) Si−Ge stretches, (2) symmetric GeH_3 wagging, (3) asymmetric GeH_3 wagging, (4) Si−Cl stretches, (5) "Si−H" rocking vibrations, (6) intense Si−H wagging, (7) asymmetrical GeH_3 rocking motion, (8) symmetrical "Ge−H" wagging motions, and (9) "SiH_2" scissor-like vibrations. As expected the latter peaks are only present in molecules containing the SiH_2 moiety (Cl-1 and Cl-2c). The feature labeled β corresponds to individual "Si−H" wagging vibrations and is predicted to shift systematically to lower frequency as the symmetry of the Cl distribution along the molecular backbone increases (e.g., along the sequence Cl-1, Cl-2a, Cl-2b, Cl-2c). Finally, the minor feature near 550 cm^{-1} labeled α is indentified as the Si−Si stretching mode and occurs as a single feature in the Cl-2a molecule and a split peak in Cl-2c. The high-frequency hydrogen stretching bands in the 2000−2300 cm^{-1} range exhibit the expected behavior with respect to the Cl substitutions. In our unscaled simulated spectra the Si−H stretch bands are centered around 2200 cm^{-1} and exhibit splittings only in the molecules containing the SiH_2 moiety (Cl-1 and Cl-2c). The Ge−H stretching bands spanning ∼2100−2170 cm^{-1} have a slightly more complex structure with the simplest peak structure occurring in the most symmetric dichlorinated molecules (Cl-2b and Cl-2c), as expected.

The simulated spectra of the Cl-2a, Cl-2b, and Cl-2c mixture were obtained using a procedure developed in our earlier work which described similar admixtures involving the pure hydride $(SiH_2)_2(H_3Ge)_2$ compound and its positional isomer $SiH(SiH_3)(GeH_3)_2$. The theoretical spectrum of the mixture is essentially obtained by minimizing an objective function[3] with respect to a combination of the three individual theoretical spectra of Cl-2a, Cl-2b, and Cl-2c. The result of this optimization process produces a spectrum which closely matches the experimental spectrum and yields a nominal admixture of 14%, 14%, and 72% for Cl-2a, Cl-2b, and Cl-2c, respectively. A comparison between the experimental spectrum and this simulation is shown at the bottom panel of Figure 4.

G. Simulation of Structural and Thermochemical Properties. The ground-state structures and vibrational and thermochemical properties of all molecules shown in Figure 5 were obtained using density functional theory at the B3LYP level using the 6-311N++G(3df,3pd) basis set, as imple-

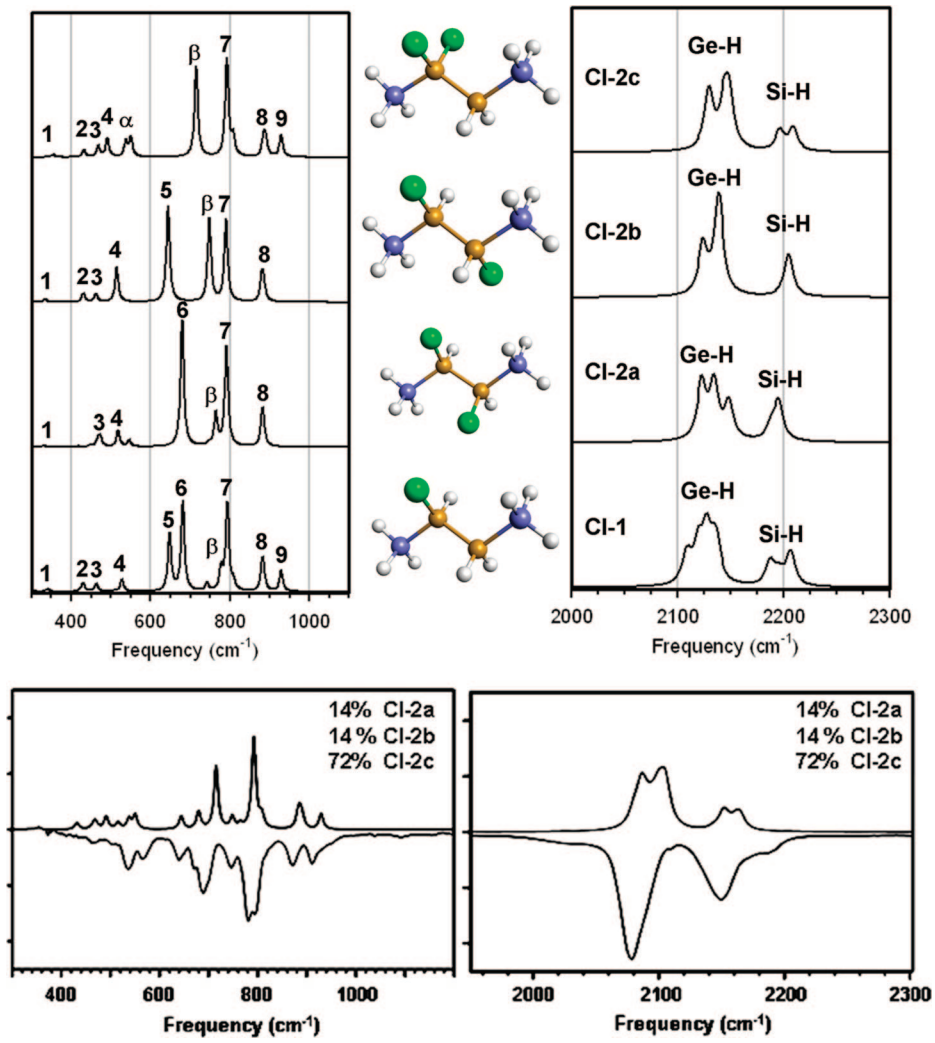

Figure 4. (Top) Unscaled simulated spectra for the mono- and dichlorinated butane-like sequence. (Bottom) Comparison of calculated and observed room-temperature IR spectra for the dichlorinated butane-like products. The theoretical spectrum corresponds to a ~3:1 mixture of the $H_3GeSiH_2SiCl_2GeH_3$ (Cl-2c) and $H_3GeSiHClSiHClGeH_3$ species (Cl-2a + Cl-2b). Frequency scale factors of 0.989 and 0.979 were applied to the calculated low- and high-frequency spectra in the top panels.

mented in the Gaussian03 program.[14] In all cases no symmetry constraints were imposed during the optimization step, and an analysis of the converged structures yields the corresponding point group symmetries provided in the figure and discussed earlier in our paper. As a point of reference we also calculated the properties of the parent propane-like $H_3Ge-SiH_2-GeH_3$ and butane-like $H_3Ge-SiH_2-SiH_2-GeH_3$ molecules (not shown). Both of these molecules exhibit a vanishing dipole moment, whereas our simulations show that chlorination produces significant dipole moments comparable to that of water (~1.85 D) in almost all cases. An exception is the $H_3Ge-SiClH-SiClH-GeH_3$ molecule whose C_i symmetry precludes formation of a static dipole moment. In liquid form these compounds are therefore expected to exhibit hydrogen-bonding behavior and properties characteristic of typical dipolar fluids. Due to the large mass of the chlorine atom, halogenation also has a profound effect on the static structural and vibrational properties of the molecules; the latter were discussed in more detail earlier in the paper. Here we discuss the effect of chlorination upon the structure of the molecules. In the three-center propane-like $ClHSi(GeH_3)_2$ (**1**) and $Cl_2Si(GeH_3)_2$ (**2**) molecules the presence of additional chlorine atoms leads to an opening of the Ge−Si−Ge angle relative to its value in the parent $SiH_2(GeH_3)_2$ molecule (112.5°, c.f. perfect tetrahedral of 109.5°). The smallest deviation from ideal tetrahedral structure is exhibited by the monochlorinated $ClSi(GeH_3)_3$, where the Ge−Si−Ge angle is 111.5°.

For the butane-like molecules our figure also lists the torsion angle ϕ which defines the planarity of the Ge−Si−

(14) Frisch, M. J.; Frisch, M. J.; Trucks, G. W.; Schlegel, H. B.; Scuseria, G. E.; Robb, M. A.; Cheeseman, J. R.; Montgomery, J. A., Jr.; Vreven, T.; Kudin, K. N.; Burant, J. C.; Millam, J. M.; Iyengar, S. S.; Tomasi, J.; Barone, V.; Mennucci, B.; Cossi, M.; Scalmani, G.; Rega, N.; Petersson, G. A.; Nakatsuji, H.; Hada, M.; Ehara, M.; Toyota, K.; Fukuda, R.; Hasegawa, J.; Ishida, M.; Nakajima, T.; Honda, Y.; Kitao, O.; Nakai, H.; Klene, M.; Li, X.; Knox, J. E.; Hratchian, H. P.; Cross, J. B.; Adamo, C.; Jaramillo, J.; Gomperts, R.; Stratmann, R. E.; Yazyev, O.; Austin, A. J.; Cammi, R.; Pomelli, C.; Ochterski, J. W.; Ayala, P. Y.; Morokuma, K.; Voth, G. A.; Salvador, P.; Dannenberg, J. J.; Zakrzewski, V. G.; Dapprich, S.; Daniels, A. D.; Strain, M. C.; Farkas, O.; Malick, D. K.; Rabuck, A. D.; Raghavachari, K.; Foresman, J. B.; Ortiz, J. V.; Cui, Q.; Baboul, A. G.; Clifford, S.; Cioslowski, J.; Stefanov, B. B.; Liu, G.; Liashenko, A.; Piskorz, P.; Komaromi, I.; Martin, R. L.; Fox, D. J.; Keith, T.; Al-Laham, M. A.; Peng, C. Y.; Nanayakkara, A.; Challacombe, M.; Gill, P. M. W.; Johnson, B.; Chen, W.; Wong, M. W.; Gonzalez, C.; Pople, J. A. *Gaussian 03*, Revision B.04; Gaussian Inc.: Wallingford, CT, 2004.

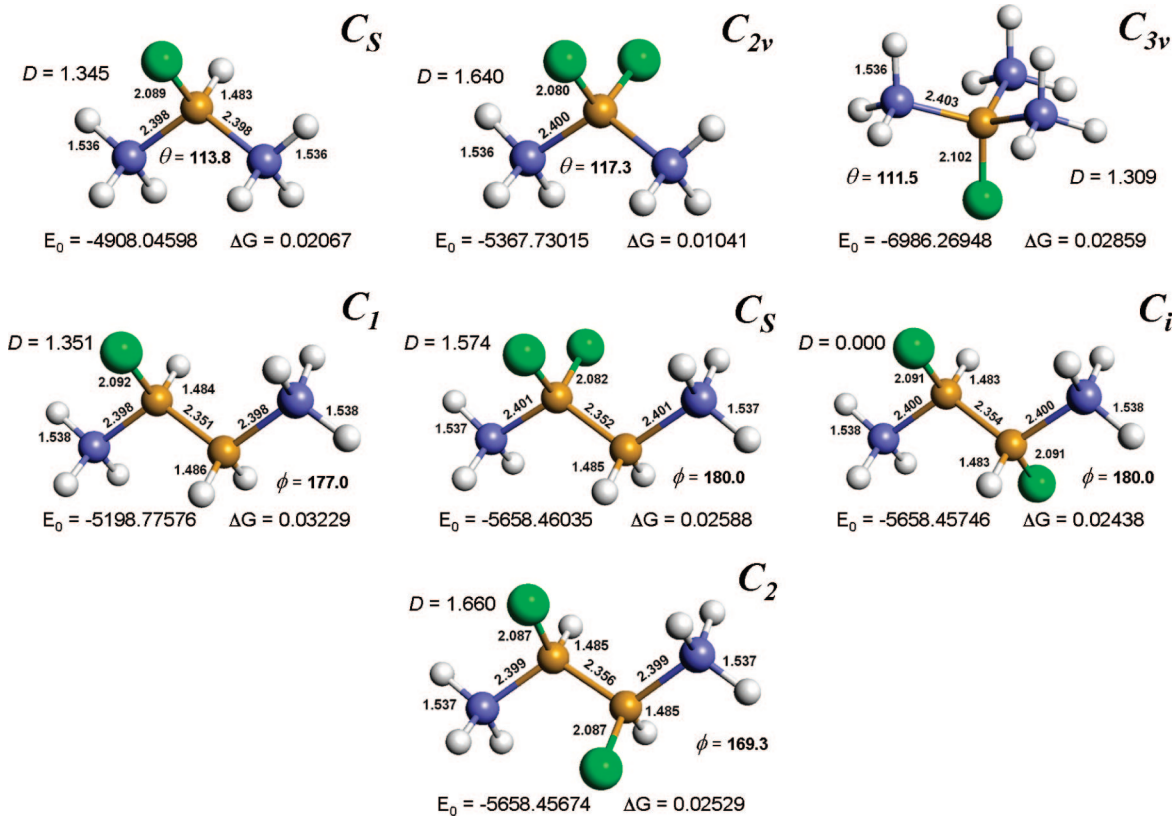

Figure 5. Structural representations of the mono- and dichlorinated propane-like and butane-like molecules. In each case the point group symmetry of the structure shown is displayed in the top right-hand corner of the panel. The figure incorporates structural and energetic data for each molecule including the dipole moment (D, in Debye units), ground-state electronic energy (E_0, in Hartree), Gibbs free energy correction at 298 K (ΔG, in Hartree), Ge−Si−Ge angles (θ, in degrees), Ge−Si−Si−Ge torsion angles (ϕ, in degrees), and bond lengths (in Angstroms). Legend: Si (gold), Ge (blue), Cl (green), and H (white).

Si−Ge backbone (planar = 180°). Deviations from planarity as large as ∼20° are predicted for the most asymmetrical chlorinated molecules, such as the $H_3Ge-SiHCl-SiHCl-GeH_3$ isomer possessing C_2 symmetry, while planarity is preserved if the chlorination occurs in a balanced fashion with respect to the backbone plane, as in the case of the $H_3Ge-SiHCl-SiHCl-GeH_3$ isomer possessing C_i symmetry, as expected. The bond-length trends are very similar to those found in all of our earlier simulation studies of the Si−Ge hydrides. The Si−Ge and Si−Si bond lengths in all molecules are calculated to be 2.400 ± 0.003 and 2.354 ± 0.003 Å, respectively. The Si−Cl bonds are generally found to lie in the range 2.082−2.092 Å, except in the $ClSi(GeH_3)_3$ molecule where a longer bond length of 2.102 Å is predicted. The more robust Si−H and Ge−H bonds exhibit a very narrow distribution with typical values of 1.484 and 1.537 Å, respectively. Finally, we list the ground-state electronic energies for all molecules (a more detailed analysis of the thermochemistry will be presented elsewhere). On the basis of the values listed the energy differences between the dichlorinated butane-like isomers suggests that binding both chlorine atoms on the same Si site is slightly preferred.

Also provided in the figure is the Gibbs free energy correction (ΔG) to E_0 at 298 K. The data indicates that the correction is enhanced in molecules possessing a large H/Cl ratio due to the prominent contribution of H to the vibrational free energy.

H. Selective Growth of $Si_{1-x}Ge_x$ Films. Next we pursued preliminary growth studies of $Si_{1-x}Ge_x$ alloys using the newly prepared chlorinated compounds to evaluate their selective-area growth potential in prototype microelectronic devices. The experiments utilized test wafers containing an array of device structures including simple transistors and various patterns masked by amorphous nitride and oxide thin layers. The depositions were conducted using gas source molecular beam epitaxy (GSMBE) at $\sim 5 \times 10^{-5}$ Torr and 380−450 °C via direct insertion of the compounds vapor pressure into the chamber held at a base pressure of 10^{-10} Torr. The film growth targeted formation of Ge-rich compositions in the range of ∼65−75%, which have applications in IR opto-electronics such as photodetectors and modulators.[15,16] The "as deposited" samples were initially examined by optical microscopy, which indicated that the color of the nitride/oxide masked regions on the surface of the wafer had remained unchanged while the color of the pure Si regions had turned from metallic gray to light brown. The latter is characteristic of high Ge content $Si_{1-x}Ge_x$, suggesting that selective deposition had potentially occurred (see Figure 6). Additional characterization of the wafers was performed by cross-sectional electron microscopy (XTEM), Raman scattering, Rutherford backscattering (RBS), and atomic force microscopy (AFM), and the data collectively revealed the presence of atomically flat Si−Ge films with single-crystalline microstructures throughout the samples. The films nominal thickness was estimated by the random RBS and

(15) Buca, D.; Winnerl, S.; Lenk, S.; Buchal, Ch.; Xu, D.-X. *Appl. Phys. Lett.* **2002**, *80* (22), 4172.

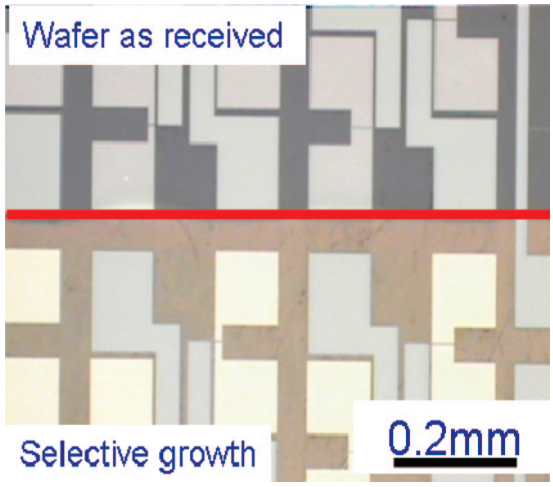

Figure 6. Optical images of selective SiGe growth on an ASM test structure. The top section of the wafer, above the red line, was shielded to block growth. Note the change in coloration between the shielded (as received) and exposed (selective growth) regions, indicating that growth has occurred selectively within well-defined areas of the pattern.

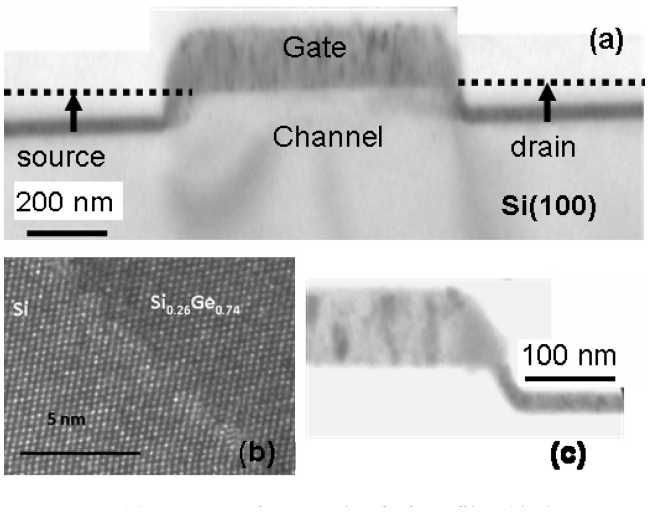

Figure 7. (a) XTEM micrograph of SiGe film (dark narrow band) grown selectively in the recessed "source" and "drain" areas of a device via deposition of $Cl_2Si(GeH_3)_2$ at 420 °C. The arrow indicates the height of the recess extending from the bottom of the trench up to the gate/channel interface (dotted line). (b) High-resolution image of the Si channel/$Si_{0.26}Ge_{0.74}$ interface, indicating commensurate growth between the two materials. (c) Enlarged view of the latter heterojunction showing that the SiGe film thickness is essentially uniform in both the sidewall and the horizontal regions.

confirmed by XTEM to be in the 50 nm range spanning the full height of the source/drain (S/D) recess region. Average growth rates up to ∼7 nm/min were obtained in these experiments. XTEM micrographs of all samples clearly demonstrated that the Si−Ge films deposited selectively and conformably on typical device structures filling the source/drain recess regions. Figure 7 shows a diffraction contrast image of a single transistor in which a 20 nm thick $Si_{0.26}Ge_{0.74}$ layer is grown selectively in the S/D regions via decomposition of $Cl_2Si(GeH_3)_2$ at 420 °C. The film thickness in this case is uniform throughout; however, note that it is significantly less than the 50 nm height of the entire recess. The latter is indicated by the length of the arrow extending from the trench bottom up to the gate/channel interface (dotted line) in Figure 7. Here the deposition process was intentionally interrupted to determine the relative growth rate of the material on the horizontal Si(100) trench bottom versus the slanted Si(111) sidewall surface. As can be seen from the bottom right-hand micrograph shown in Figure 7 the thickness is uniform, indicating that the growth likely occurred simultaneously, at the same rate, throughout the entire surface (sidewall and bottom) of the trench. Note, in particular, that no discernible growth occurred on the nitride spacers or on the masked polysilicon gate hardmask features of the structure, as expected in the case of highly selective growth behavior. The diffraction data in general reveal fully conformal and continuous layers regardless of the crystallographic orientation at the growth surface on the device platform. Furthermore, atomic resolution XTEM images revealed that the film is pseudomorphic to the Si substrate and atomically flat. AFM scans show a typical roughness of 0.5 nm, which is consistent with a layer-by-layer growth mode.

Micro-Raman spectroscopy was used to study the selectivity of growth and determine the Si−Ge composition throughout the wafer surface at a spatial resolution of ∼1 μm. The spectra of all samples obtained from the nitride/oxide covered features showed only a single peak corresponding to the Si−Si vibrations of the underlying substrate, indicating that no discernible Si−Ge growth had occurred in these areas in agreement with the XTEM observations. The Raman spectra obtained from the unprotected Si regions, however, showed three additional peaks corresponding to the characteristic Si−Si, Si−Ge, and Ge−Ge alloy vibrations, indicating significant growth of crystalline $Si_{1-x}Ge_x$ films with a composition of $Si_{0.26}Ge_{0.74}$. It is important to note that the Raman composition was obtained as an average from a large number of measurements of individual device features throughout the entire wafer and closely matched the bulk film composition obtained from RBS. The RBS/Raman results collectively suggest that precise compositional control can be achieved by selective-area deposition of our compounds. These afford low-temperature depositions that produce controllable and fairly homogeneous alloys within and among individual device architectures. This level of uniformity is critically important for achieving reliable, reproducible, and cost-effective device fabrication and performance. In addition, the use of single sources simplifies significantly the integration scheme by circumventing complex multicomponent reactions and corrosive Cl_2 etchants which are necessary to promote selective deposition in conventional processes.

In addition to selective deposition experiments we also explore the possibility of achieving highly strained states in our deposited films. Figure 8 shows a reciprocal space map (RSM) of a ∼30 nm thick $Si_{0.33}Ge_{0.67}$ layer grown by deposition of $ClHSi(GeH_3)_2$ at 420 °C at a rate of 6−8 nm/min. The composition of the film as measured by RBS closely matches that of the corresponding precursor, indicating that the entire $SiGe_2$ core is being incorporated into the material. The in-plane and vertical lattice parameters were

(16) Kuo, Y.-U.; Lee, Y.-K.; Ge, Y.; Ren, S.; Roth, J. E.; Kamins, T. I.; Miller, D. A. B.; Harris, J. S. *Nature* **2005**, *437* (7063), 1334.

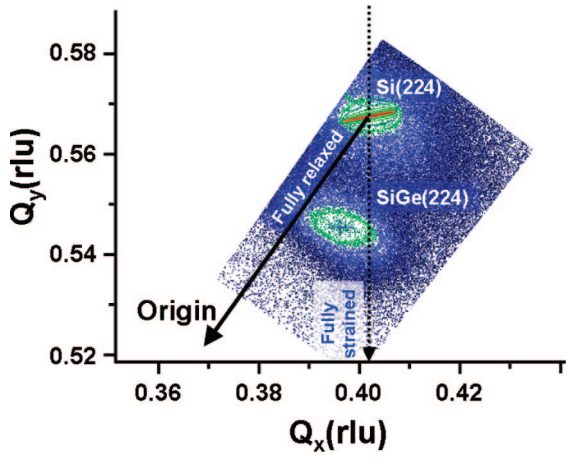

Figure 8. High-resolution XRD 2-D reciprocal space map of the (224) reflection of $Si_{0.33}Ge_{0.67}$ in reciprocal lattice units (rlu) relative to the Si peak.

determined to be 5.4986 and 5.6530 Å, respectively. Using these values and standard elasticity theory we obtain an unprecedented compressive strain of −1.6%. Note that this value is significantly higher than the 1.2% strains that are possible from state-of-the-art films containing 30% Ge. The RSM plot in Figure 8 reveals that our film is ∼40% relaxed, suggesting that it may be possible to reach fully strained films by optimizing deposition conditions such as growth rate and temperature. By reducing the temperature to 400 °C we have been able to produce films that exhibit compressive strain approaching −2.4%, which is close to the maximum value of 2.75% expected for the $Si_{0.33}Ge_{0.67}$ composition. In this case the high growth rate of 5−6 nm/min and low growth temperature "trap" highly metastable strain states in layers exhibiting a significant thickness of 20−25 nm as measured by XTEM and ellipsometry. These thicknesses far exceed the critical equilibrium value of less than ∼ 2 nm for $Si_{0.33}Ge_{0.67}$ grown on Si. Figure 9 shows XTEM micrographs of this material illustrating a uniform film thickness, a smooth surface, and a fully commensurate interface. Diffraction contrast images revealed defect-free layers within the instrument field of view spanning several micrometers. The described single-source route presented here enables for the first time facile conversion of diamond cubic Si−Ge into tetragonally structured alloys with average lattice constants of 5.451 and 5.688 Å that cannot be obtained by conventional methods. The biaxial stress σ required to tetragonally strain a free-standing film of the same material perpendicular to the (100) direction (without bending or buckling) is given by $\sigma = [C_{11} + C_{12} - 2C_{12}^2/C_{11}]\varepsilon$. Assuming a linear interpolation between the known elastic constants of pure Si and Ge, we obtain $\sigma \approx 4$ GPa for our $Si_{0.33}Ge_{0.67}$ film with a corresponding in-plane strain of 0.24%. This is approximately twice the stress recently reported for a SiGe film with 25−30% Ge possessing an in-plane strain of ∼1%.

Conclusions

Selective chlorination of $SiH_2(GeH_3)_2$, $SiH(GeH_3)_3$, and $(SiH_2)_2(GeH_3)_2$ was achieved by low-temperature reaction with BCl_3 to yield $ClHSi(GeH_3)_2$ (**1**), $Cl_2Si(GeH_3)_2$ (**2**), $ClSi(GeH_3)_3$ (**3**), and $ClHSiSiH_2(GeH_3)_2$ (**4**). The bonding structure and vibrational properties of all compounds were systematically characterized using a combination of NMR, FTIR, mass spectroscopy, and density functional theory molecular simulations. The second chlorination of the butane-like analogs produced ∼3:1 mixtures of $Cl_2SiSiH_2(GeH_3)_2$ and $(ClHSi)_2(H_3Ge)_2$ isomers, respectively. The relative proportions were determined by fitting the observed FTIR spectrum of the mixture to a superposition of individual isomer FTIR spectra obtained from simulation. As a proof-of-principle demonstration of the utility of the $Cl_2Si(GeH_3)_2$ as a single-source precursor for selective low-temperature growth of Ge-rich semiconductor films, we deposited homogeneous, stoichiometric, and highly crystalline $Si_{0.26}Ge_{0.74}$ semiconductor alloy in the "source" and "drain" region of a simple transistor structure.

Experimental Section

General Methods. All manipulations were carried out under inert conditions using standard high-vacuum line and drybox techniques. Dry, air-free solvents were distilled from either anhydrous $CaCl_2$ or sodium benzophenone ketyl prior to use. The NMR spectra were collected on either a Varian Inova 500 MHz or a Varian 800 MHz spectrometer. Samples were dissolved in deuterated benzene, and all nuclei were referenced either directly or indirectly to the signal of TMS or the residual solvent peak as indicated. Gaseous IR spectra were obtained in 10 cm cells fitted with KBr windows. Mass spectrometry data were obtained using an Extorr mass spectrometer. Boron trichloride (Aldrich 99.95%) was distilled to remove residual HCl contaminants, and its purity was confirmed by infrared and mass spectra prior to use. Lithium tetrahydroaluminate (Aldrich), phenyl trichlorosilane (Aldrich), chloro(*p*-tolyl)silane (Gelest), trifluoromethane sulfonic acid (Alfa Aesar), nonafluorobutane-1-sulfonic acid (Aldrich), diphenylsilane (Gelest), triphenylsilane (Gelest), and electronic-grade germane gas (donated by Voltaix, Inc.) were used as received. The starting materials digermylsilane,[1] trigermylsilane,[1] and digermyldisilane[3] were all prepared according to their literature procedures and checked by NMR spectroscopy to verify their purities prior to use. Potassium germyl ($KGeH_3$) was synthesized via a modified literature preparation in monoglyme by reaction of gaseous GeH_4 with a finely dispersed sodium−potassium (80% K) alloy. Note: the Teflon bar that was used to stir the GeH_4/Na−K/monoglyme solution was encapsulated in glass owing to the high reactivity of Teflon with Na−K alloys.

Reaction of 1:3 $BCl_3/SiH_2(GeH_3)_2$. Gaseous BCl_3 (0.12 g, 1.05 mmol) and $SiH_2(GeH_3)_2$ (0.57 g, 3.14 mmol) were condensed into a 50 mL round-bottom flask. The flask and its contents were held at 0 °C for 2 h, after which time the volatiles were passed through U traps held at −40, −60, and −196 °C. The latter contained B_2H_6 (0.5 mmol, 100% yield) and a minor amount of starting material as evidenced by gas IR spectroscopy. The −60 °C trap contained pure **1** as a clear, colorless liquid. The −40 °C trap contained a mixture of **1** and **2** as evidenced by ^{1}H NMR. The yields for **1** and **2** were found to be 0.38 (36%) and 0.03 mmol (3%), respectively. Pure compound **1** was obtained by additional distillation.

*$ClHSi(GeH_3)_2$ (**1**).* IR (gas, cm^{-1}): 2153 (m), 2088 (s), 2075 (s), 880 (s), 793 (s), 767 (vs), 697 (vs), 573 (w), 549 (w), 469 (w), 411 (vw). ^{1}H NMR (500 MHz, C_6D_6): δ 5.07 (septet, H, J = 3.5 Hz, SiH), 3.28 (d, 6H, J = 3.5 Hz, Ge−H_3). ^{29}Si (500 MHz, C_6D_6): δ −14.71. Mass spectrum: m/z isotopic envelopes centered at 207 (M^+), 172 ($SiGe_2H_x^+$), 144 ($Ge_2H_x^+$), 141 ($ClSiGeH_x^+$), 101 ($SiGeH_x^+$), 73 (GeH_x^+), 63 ($ClSiH_x^+$), 36 (Cl^+), 29 (SiH_x^+).

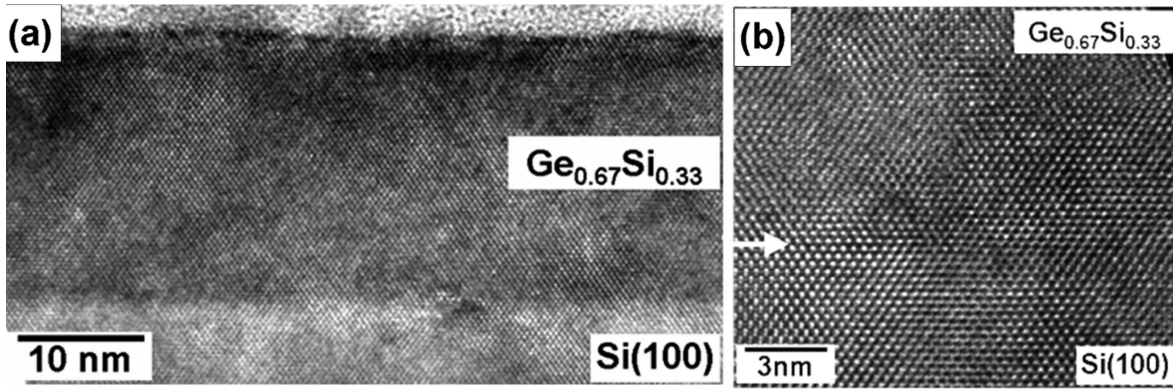

Figure 9. (a) XTEM high-resolution micrograph of a 22 nm thick $Si_{0.33}Ge_{0.67}$ film exhibiting a compressive strain of −2.4%. (b) Enlarged area of the interface region showing perfect epitaxial registry between the film and substrate.

Reaction of 2:3 BCl_3:$SiH_2(GeH_3)_2$. BCl_3 (0.23 g, 1.97 mmol) and $SiH_2(GeH_3)_2$ (0.53 g, 2.95 mmol) were condensed into a 50 mL round-bottom flask. The flask and its contents were held at 0 °C for 1 h, after which time the volatiles were passed through traps held at −40, −78, and −196 °C. The −196 °C trap contained pure B_2H_6 as evidenced by IR spectroscopy. The −78 °C trap contained pure **1** as evidenced by IR spectroscopy. The −40 °C trap contained a mixture of **1** and **2**. Integration of the Ge−H peaks in the ^{1}H NMR spectrum showed a 3:2 ratio of $ClHSi(GeH_3)_2$:$Cl_2Si(GeH_3)_2$. Overall, 0.62 mmol (21% yield) of **1** and 0.38 mmol (13% yield) of **2** were obtained.

Reaction of 1:1 BCl_3:$SiH_2(GeH_3)_2$. BCl_3 (0.086 g, 0.74 mmol) and $SiH_2(GeH_3)_2$ (0.13 g, 0.74 mmol) were condensed into a 50 mL round-bottom flask. The flask and its contents were held at 0 °C for 30 min, after which time the volatiles were passed through traps held at −40, −78, and −196 °C. The latter contained B_2H_6 as evidenced by IR spectroscopy. The −78 °C trap contained pure **1** (0.007 mmol, 1% yield). The −40 °C trap contained pure **2** as a clear, colorless liquid (0.15 mmol, 20% yield).

*$Cl_2Si(GeH_3)_2$ (**2**).* Vapor pressure: 7 torr (23 °C). IR (gas, cm^{-1}): 2088 (vs), 2077 (s), 880 (m), 796 (s), 767 (vs), 572 (w), 551 (w), 472 (w). ^{1}H NMR (500 MHz, C_6D_6): δ 3.42 (s, 6H, Ge−H_3). ^{29}Si (500 MHz, C_6D_6): δ 30.22. Mass spectrum: *m/z* isotopic envelopes centered at 246 (M^+), 208 ($ClSiGe_2H_x^+$), 178 ($Cl_2SiGeH_x^+$), 171 ($SiGe_2H_x^+$), 145 ($Ge_2H_x^+$), 141 ($ClSiGeH_x^+$), 128 ($ClSiGeH_x^+$), 103 ($Cl_2SiH_x^+$), 100 ($SiGeH_x^+$), 75 (GeH_x^+), 65 ($ClSiH_x^+$), 36 (Cl^+), 29 (SiH_x^+).

Synthesis of $ClSi(GeH_3)_3$. A 25 mL round-bottom flask was charged with $(GeH_3)_3SiH$ (0.46 g, 1.8 mmol), and BCl_3 (0.21 g, 1.8 mmol) was subsequently condensed into the flask. The flask and its contents were maintained at 0 °C for 10 min, after which time the volatiles were passed through traps at temperatures of −78 and −196 °C. The −196 °C trap contained B_2H_6 (0.9 mmol, 100% yield) as evidenced by IR spectroscopy. The −78 °C trap contained pure **3** as a clear, colorless liquid (0.36 mmol, 19% yield).

*$ClSi(GeH_3)_3$ (**3**).* Vapor pressure: 2 torr (23 °C). IR (gas, cm^{-1}): 2082 (s), 2071 (s), 2065 (s), 787 (w), 770 (vs), 680 (vw), 551 (vw), 466 (w). ^{1}H NMR (500 MHz, C_6D_6): δ 3.49 (s, 9H, Ge−H_3). ^{29}Si (500 MHz, C_6D_6): δ −8.13. Mass spectrum: *m/z* isotopic envelopes centered at 284 (M^+), 247 ($SiGe_3H_x^+$), 217 ($Ge_3H_x^+$), 208 ($ClSiGe_2H_x^+$), 177 ($SiGe_2H_x^+$), 147 ($Ge_2H_x^+$), 135 ($ClSiGeH_x^+$), 107 ($SiGeH_x^+$), 74 (GeH_x^+), 64 ($ClSiH_x^+$), 36 (Cl^+), 29 (SiH_x^+).

Reaction of 2:3 BCl_3:$(SiH_2)_2(GeH_3)_2$. A 25 mL round-bottom flask was charged with $(GeH_3)_2(SiH_2)_2$ (0.20 g, 0.95 mmol), and BCl_3 (0.07 g, 0.63 mmol) was subsequently condensed into the flask. The flask and its contents were held at 0 °C for 1 h, after which time the volatiles were distilled through traps at −20, −50, and −196 °C. The −196 °C trap contained B_2H_6 as evidenced by gas IR spectroscopy. The −50 °C trap contained $ClHSiSiH_2(GeH_3)_2$ and unreacted starting material, while the −20 °C trap retained pure $ClHSiSiH_2(GeH_3)_2$ as a clear, colorless liquid.

*$ClHSiSiH_2(GeH_3)_2$ (**4**).* Vapor pressure: 1.5 torr (23 °C). IR (gas, cm^{-1}): 2152 (s), 2137 (s), 2076 (vs), 2072 (vs), 2065 (m), 916 (m), 880 (w), 801 (s), 744 (w), 686 (s), 654 (m), 539 (vw), 471 (vw), 439 (vw).[1] ^{1}H NMR (500 MHz, C_6D_6): δ 3.05 (t, 3H, Ge−H_3), δ 3.26 (d, 3H, Ge−H_3), δ 3.33 (pentet, 2H, Si−H_2), δ 5.02 (sextet, H, Si−H). ^{29}Si (500 MHz, C_6D_6): δ −97.0 (Si−H_2), −15.0 (Si−HCl).

Reaction of 1:1 BCl_3:$(SiH_2)_2(GeH_3)_2$. A 25 mL round-bottom flask was charged with $(SiH_2)_2(GeH_3)_2$ (0.26 g, 1.3 mmol), and BCl_3 (0.15 g, 1.3 mmol) was subsequently condensed into the flask. The flask and its contents were held at 0 °C for 20 min, after which time the volatiles were distilled through traps at −15 and −196 °C. The −196 °C trap contained B_2H_6 as evidenced by gas IR spectroscopy. The −15 °C trap contained a clear colorless liquid with a vapor pressure of 0.5 torr, which was characterized by IR and NMR to be a mixture between $(ClHSi)_2(H_3Ge)_2$ and $Cl_2SiSiH_2(GeH_3)_2$. Vapor pressure: 0.8 torr (23 °C). IR (gas, cm^{-1}): 2152 (s), 2137 (s), 2076 (vs), 2072 (vs), 2065 (m), 910 (m), 872 (w), 795 (s), 782 (s), 748 (w), 690 (s), 672 (w), 641 (m), 566 (m), 537 (m), 508 (vw), 484 (vw), 463 (vw), 424 (vw).

$(ClHSi)_2(H_3Ge)_2$. ^{1}H NMR (500 MHz, C_6D_6): δ 3.26 (d, 6H, Ge−H_3), 4.98 (pentet, H, Si−H). ^{29}Si (500 MHz, C_6D_6): δ −17.0.

$Cl_2SiSiH_2(GeH_3)_2$. ^{1}H NMR (500 MHz, C_6D_6): δ 3.43 (s, 3H, Ge−H_3), 3.42 (q, 2H, Si−H_2), 3.07 (t, 3H, Ge−H_3). ^{29}Si (500 MHz, C_6D_6): δ −88.7 (Si−H_2), 24.4 (Si−Cl_2)

Acknowledgment. This research was supported by the U.S. Air Force Office of Scientific Research (AFOSR MURI, FA9550-06-01-0442), Voltaix Corporation, and the NSF (IIP 053950). The XRD equipment used in this work was obtained by a grant from the NSF (DMR-0526604). We thank Dr. V. R. D'Costa for help with preliminary Raman characterization.

CM800427P